Assessment of spatio-temporal gait parameters from trunk accelerations during human walking

Zijlstra, W; Hof, AL

Published in:
Gait & Posture

Publication date:
2003

Available online at www.sciencedirect.com
SCIENCE DIRECT®
Gait and Posture 18 (2003) 1–10
GAIT & POSTURE
www.elsevier.com/locate/gaitpost

Assessment of spatio-temporal gait parameters from trunk accelerations during human walking

Wiebren Zijlstra *, At L. Hof

Institute of Human Movement Sciences, University of Groningen, P.O. Box 196, 9700 AD Groningen, The Netherlands

Received 19 September 2002; received in revised form 10 October 2002; accepted 17 October 2002

Abstract

This paper studies the feasibility of an analysis of spatio-temporal gait parameters based upon accelerometry. To this purpose, acceleration patterns of the trunk and their relationships with spatio-temporal gait parameters were analysed in healthy subjects. Based on model predictions of the body's centre of mass trajectory during walking, algorithms were developed to determine spatio-temporal gait parameters from trunk acceleration data. In a first experiment, predicted gait parameters were compared with gait parameters determined from ground reaction forces measured by a treadmill. In a second experiment, spatio-temporal gait parameters were determined during overground walking. From the results of these experiments, it is concluded that, in healthy subjects, the duration of subsequent stride cycles and left/right steps, and estimations of step length and walking speed can be obtained from lower trunk accelerations. The possibility to identify subsequent stride cycles can be the basis for an analysis of other signals (e.g. kinematic or muscle activity) within the stride cycle.

Keywords: Locomotion; Accelerometry; Ambulatory measurements; Foot contact detection; Inverted pendulum model

1. Introduction

Basic prerequisites for gait analysis are the assessment of spatio-temporal gait parameters and the analysis of movements within subsequent stride cycles. This parameterisation of gait requires the detection of subsequent foot contacts. Not only is foot contact detection important for the determination of essential spatio-temporal gait characteristics (e.g. step length or stride duration), also the analysis of kinematic or physiologic signals during subsequent stride cycles critically depends on the detection of onset and end of stride cycles. As a matter of convention, the stride cycle is defined as the interval between two subsequent right foot contacts. Hence, the stride starts with a left step, which is followed by a right step. In laboratory experiments, the identification of subsequent stride or step cycles is usually not a problem; several methods exist to detect foot contacts. Some typical examples are the use of conducting foot switches [1], pressure-sensitive foot switches [2–4], ground reaction forces (GRFs) [5,6], or the analysis of foot displacement patterns [7,8]. However, these methods are often impractical or even impossible to use when gait is studied under real-life conditions, e.g. by using body-fixed sensors and ambulatory equipment or telemetry. Indeed, methods for ambulatory gait measurements must meet a number of demands. Not only must the validity of methods be demonstrated, the methods must preferably also be easy-to-use and non-obtrusive.

Although already in the 1970s the use of accelerometers for an analysis of human movement was suggested [9], it is only recently that a number of studies have reported gait analyses based upon the use of accelerometers on trunk, thigh, shank or foot (for examples see Refs. [10–12]). Only few studies have addressed the relationships between measured accelerations and spatio-temporal gait parameters. Using neural networks, the speed and distance of walking can be estimated [13]. Average temporal characteristics like step or stride duration can be estimated from acceleration data (for example, by means of cross correlation

* Corresponding author. Tel.: +31-50-363-7868; fax: +31-50-363-3150
E-mail address: w.zijlstra@med.rug.nl (W. Zijlstra).

0966-6362/02/$ - see front matter
PII: S0966-6362(02)00190-X

functions or frequency analysis). However, these approaches do not yield an exact identification of individual stride cycles such as required for the analysis of mean electromyography (EMG) signals or angular joint movements. Successive foot contacts can be detected from accelerations of the thigh, foot or shank [14,15]. However, this detection is not always easy [15], and, even if foot contacts are successfully detected, it may not always be possible or practical to mount accelerometers on both legs.

A recent study by Zijlstra and Hof [16] suggests that during walking a basic pattern of trunk accelerations with fixed relationships to spatio-temporal gait parameters can be expected. Their study demonstrated that three-dimensional (3D) displacements of the lower trunk during walking are predicted well by an inverted pendulum model of the body's centre of mass (CoM) trajectory [16]. In agreement with model predictions, the amplitude and timing of pelvic displacements depended on spatio-temporal parameters of the stride cycle. The inverted pendulum model also predicts a basic pattern of lower trunk acceleration during walking, and relationships between acceleration characteristics and spatio-temporal gait parameters. Hence, spatio-temporal gait parameters can possibly be determined from accelerations of the lower trunk. Therefore, the present paper investigates the feasibility of an analysis of spatio-temporal gait parameters based upon accelerometry. Specifically, it analyses the 3D-acceleration pattern of the lower trunk at different walking speeds, and it evaluates algorithms that were developed to determine the instant of foot contacts, to identify left and right foot contacts, and to estimate mean step length and walking speed.

2. Methods

The relationships between 3D accelerations of the lower trunk and spatio-temporal gait parameters were evaluated by means of analyses of treadmill walking in 15 subjects and overground walking in 10 subjects. None of the participants suffered from a disease or trauma that could interfere with their regular walking pattern. The local ethics committee has approved the study, and subjects participated after giving their informed consent.

2.1. Subjects and conditions

Eight male and seven female subjects participated in the treadmill walking experiment. Their age ranged from 21 to 27 years (mean: 22.9 years), their body mass ranged from 58 to 93 kg (mean: 76.9 kg), and their leg length ranged from 0.90 to 1.10 m (mean: 1.005 m). As this group of subjects included persons with and persons without previous experience of treadmill walking, all subjects were familiarised with treadmill walking by test walks at different speeds. After getting accustomed to treadmill walking, measurements were made at the following treadmill speeds: 0.5, 0.75, 1.0, 1.25, 1.5 and 1.75 m/s.

Overground walking was studied in five male and five female subjects who did not participate in the treadmill walking experiment. Their age ranged from 21 to 25 years (mean: 23.3 years), their body mass ranged from 64 to 89 kg (mean: 76.3 kg), and their leg length ranged from 0.86 to 1.12 m (mean: 0.978 m). After a test walk to get accustomed to the experimental procedure, these subjects were asked to walk along an approximately 60-m long passage in a public building. Measurements were made at their preferred speed and at a slow and a fast speed. Since other visitors to the building were present, subjects could encounter other persons while a measurement was made. This was accepted as long as the subject did not need to abruptly correct his or her gait trajectory.

In both experiments, subjects walked on regular shoes wearing their usual clothing. Measurements of body mass and leg length (defined as the distance between the ground and the top of right trochanter major femoris) were made with clothes and shoes on.

2.2. Data acquisition

In both experiments, accelerations of the lower trunk were measured by a tri-axial accelerometer (Kistler; sensitivity: 500 mV/g, range: ± 2 g). This accelerometer is a DC-type sensor, which is also sensitive to acceleration due to gravity. The accelerometer was solidly attached to a small, lightweight plate with elastic (neoprene) bandages attached to it. With the bandages firmly strapped around the pelvis, the accelerometer was positioned at the dorsal side of the trunk. The heart of the accelerometer was approximately at the level of the second sacral vertebrae. With the subject standing in anatomical position, the orientation of the accelerometer was conform ISB recommendations [17], i.e. positive X values correspond to anterior acceleration, positive Y values to upward acceleration, and positive Z values to an acceleration to the right.

For the treadmill walking experiments, a treadmill was used which was based on a treadmill used by Verkerke et al. [6]. The treadmill was equipped with force transducers underneath a left and a right walking surface. Vertical GRFs were calculated by summation of the force transducer signals under each walking surface. Data of the force transducers and the accelerometer were sampled at 100 Hz. Duration of a measurement was 30 s at all speeds. Measurements were made after the subject had walked on the specific speed for at least 30 s. After a measurement, treadmill speed was in-

creased and after at least 30 s, the next measurement was made.

During the overground walking trials, accelerometer data were sampled at 100 Hz by an ambulatory measurement system. In addition, an observer marked the instants where a subject passed the start or end of a 25-m distance along the trajectory by pushing a button, thus producing a signal that was recorded on an extra marker channel.

In both the experiments, all data were low-pass filtered before further analysis (fourth-order zero-lag Butterworth filter at 20 Hz).

2.3. Analysis of treadmill walking data

GRF data and acceleration data were analysed as follows.

Onsets of support phases were determined by three different methods: from left and right GRFs, and from forward accelerations. In the GRF method, the onset of a support phase was taken as the instant when the left or right GRF exceeded a threshold of 6.5% of body weight. The two other methods use the characteristic pattern of trunk acceleration during walking. Based on an inverted pendulum model as described in Ref. [16], the shape of the acceleration signal can roughly be predicted. During single support, an increase in forward acceleration can be expected when, after mid-stance, the body is falling forward and downward. During the transition from single to double support (i.e. after contralateral foot contact), the forward fall of the body changes into an upward movement in which the forward movement decelerates. Thus, foot contact should coincide with a change of sign of the forward acceleration of the lower trunk. One procedure for foot contact detection, the zero-crossing method, is based on this expectation. After low-pass filtering the forward acceleration signal (fourth-order zero-lag Butterworth filter), the switch from positive to negative was taken as the instant of a foot contact. In a refinement of this method, the peak forward acceleration preceding the change of sign (as determined by the zero-crossing method) is taken as the instant of foot contact. In both approaches, a cut-off frequency of 2 Hz was chosen based upon the expected maximum step rate, i.e. a maximum step frequency of approximately 2 Hz at a treadmill speed of 1.75 m/s (see Ref. [16]). The results of the GRF method versus those of the zero-crossing method and peak detection method were compared by calculating differences between data sets. To this purpose, 10 stride cycles (i.e. 20 steps) were used for each subject and each belt speed condition. Mean differences and root mean square (RMS) values were calculated from group data (i.e. more than 300 foot contacts) at each belt speed.

The pattern of accelerations within the stride cycle was analysed by calculating ensemble averages of the accelerations. To this purpose, stride cycles (as identified from right GRFs) were time-normalised on a scale of 0–100%. For each subject, mean acceleration patterns were calculated from 10 stride cycles per condition.

Discrimination between left and right steps was based upon an analysis of mediolateral movements of the lower trunk. Experimental data [16,18,19] and model predictions [16] have shown that the CoM, and consequently also the lower trunk, describes an approximately sinusoidal path between the medial borders of the feet during subsequent foot placements. Using the inverted pendulum model described in Ref. [16], it is predicted that the CoM accelerates to the left during a right support phase and to the right during a left support phase. During single support, the CoM reaches its maximum lateral position towards the stance leg. Hence, discrimination of left and right foot contacts can possibly be based on mediolateral acceleration or position data. We chose to use position rather than acceleration data. Changes in mediolateral position were calculated by a double integration of Z. To avoid integration drift, position data were high-pass filtered (fourth-order zero-lag Butterworth filter at 0.1 Hz). Identical to Ref. [16], the first harmonic was used to describe amplitude and timing of the left–right displacement pattern during a stride cycle. At each foot contact, a stride cycle was defined as the interval between the preceding and following foot contact. Subsequently, the amplitude and phase of the first harmonic were calculated. This procedure resulted in different phases around left and right foot contacts. Thus, the phase of the first harmonic could be used to distinguish left from right. The results of this procedure were compared with the left and right foot contacts as identified by the GRF method.

Mean step length and mean walking speed were estimated using the upward and downward movements of the trunk. Assuming a compass gait type, CoM movements in the sagittal plane follow a circular trajectory during each single support phase. In this inverted pendulum model, changes in height of CoM depend on step length [16]. Thus, when changes in height are known, step length can be predicted from geometrical characteristics as follows:

$$\text{step length} = 2\sqrt{2lh - h^2}.$$

In this equation, h is equal to the change in height of the CoM, and l equals pendulum length. Changes in vertical position were calculated by a double integration of Y. To avoid integration drift, position data were high-pass filtered (fourth-order zero-lag Butterworth filter at 0.1 Hz). The amplitude of changes in vertical position (h) was determined as the difference between highest and lowest position during a step cycle. Leg length was taken as pendulum length (l). From these data, step lengths

were estimated. After step lengths were estimated for 20 subsequent steps, a mean step length was calculated. From the same 20 steps, mean step duration was calculated. For each subject and each belt speed condition, mean step length divided by mean step duration was used to estimate walking speed.

2.4. Analysis of overground walking

For each subject and each trial, mean walking speed was calculated from the time it took for the subject to cross the 25-m distance along the trajectory. Per trial, all acceleration data measured between the recorded marker signals were used for further analysis. Thus, depending on walking speed, the amount of data differed per subject and trial. Trunk acceleration data were used to determine the instants of left and right foot contacts and to estimate step length and walking speed. To this purpose, identical algorithms were used as those developed for analysing the treadmill walking data. To evaluate the algorithms, estimated walking speeds were compared to the calculated mean walking speeds.

3. Results

3.1. Accelerations of the lower trunk during treadmill walking

Fig. 1 shows mean acceleration data of a representative subject during walking at different treadmill speeds. Although differences were observed between subjects, some basic features of the 3D-acceleration pattern could be observed. First of all, accelerations in forward and upward directions show a pattern that is related to the step cycle. In Fig. 1, it can be seen that the pattern from 0 to 50% of the stride cycle repeats itself from 50 to 100%. The left–right accelerations are also related to the step cycle, but the pattern during the first part of the stride cycle (i.e. a left step) is mirrored during the second part (i.e. a right step). Despite between-subject variation in the patterns and small asymmetries between left and right steps, these basic features were observed in all subjects and at all speeds. Secondly, an effect of walking speed could be observed in all movement directions. In general, the acceleration patterns were similar at different speeds, but they became more pronounced because of an increase in peak amplitudes. The latter increases were most prominent in antero-posterior and vertical accelerations.

Antero-posterior acceleration data show a basic pattern of acceleration and deceleration; at foot contact (i.e. at 0 and 50% of the stride cycle) forward acceleration reaches peak values, and after foot contact a sharp decline is followed by a period of deceleration. This decline becomes steeper with increasing speed. The basic pattern was observed in all subjects. However, in some subjects we observed additional acceleration peaks which varied from cycle to cycle and also with walking speed. Closer inspection of these acceleration signals in relation to the GRF data showed that the timing of an additional peak or indention corresponded to the beginning or end of swing phases, respectively. In the mean data presented in Fig. 1, such an indention can be observed just preceding the peak acceleration at 50% of the stride cycle. The indention preceding foot contact could cause a short period of negative values in forward acceleration.

On average, vertical accelerations are equal to the acceleration due to gravity (9.81 m/s^2). In Fig. 1, this mean acceleration has been subtracted from the vertical acceleration data. The vertical acceleration pattern shows a basic pattern of acceleration and deceleration. Values lower than gravity are found during mid-stance (approximately at 25 and 75% of the stride cycle). These values are compensated for by an upward acceleration (i.e. values larger than gravity) which starts at the end of the step cycle and lasts until the first part of the single support phase. In most subjects, a short period of decrease in upward acceleration can be observed at the ends of double support phases (i.e. approximately 10–15% after foot contacts). At these moments, acceleration may reach values lower than gravity. The amplitudes of maximal acceleration and deceleration become larger with increasing walking speed. These observations are representative for the whole group of subjects.

During right support phase, the major part of the mediolateral acceleration was to the left, and vice versa. Generally, these accelerations are of small amplitude. However, around foot contacts, acceleration peaks and deviations from the basic pattern occurred, and generally, the patterns of mediolateral accelerations show more between-subject variation than forward accelerations. Within subjects, the individual pattern was consistent at different speeds.

3.2. Foot contact detection and duration of the stride cycle

Fig. 2 illustrates the three methods of foot contact detection. The upper figure marks the detected foot contacts in combination with forward acceleration data. The lower figure shows vertical GRFs during left and right support phases. As can be observed in the figure, the methods resulted in differences in timing. Generally, the comparison of the GRF method (marked by asterisks) versus the peak detection method (open circles) shows a close correspondence of data, whereas the zero-crossing method (marked by a downward slope of the block signal) always resulted in a later detection of foot contacts than detection from GRF data. The differences between methods were quantified; together

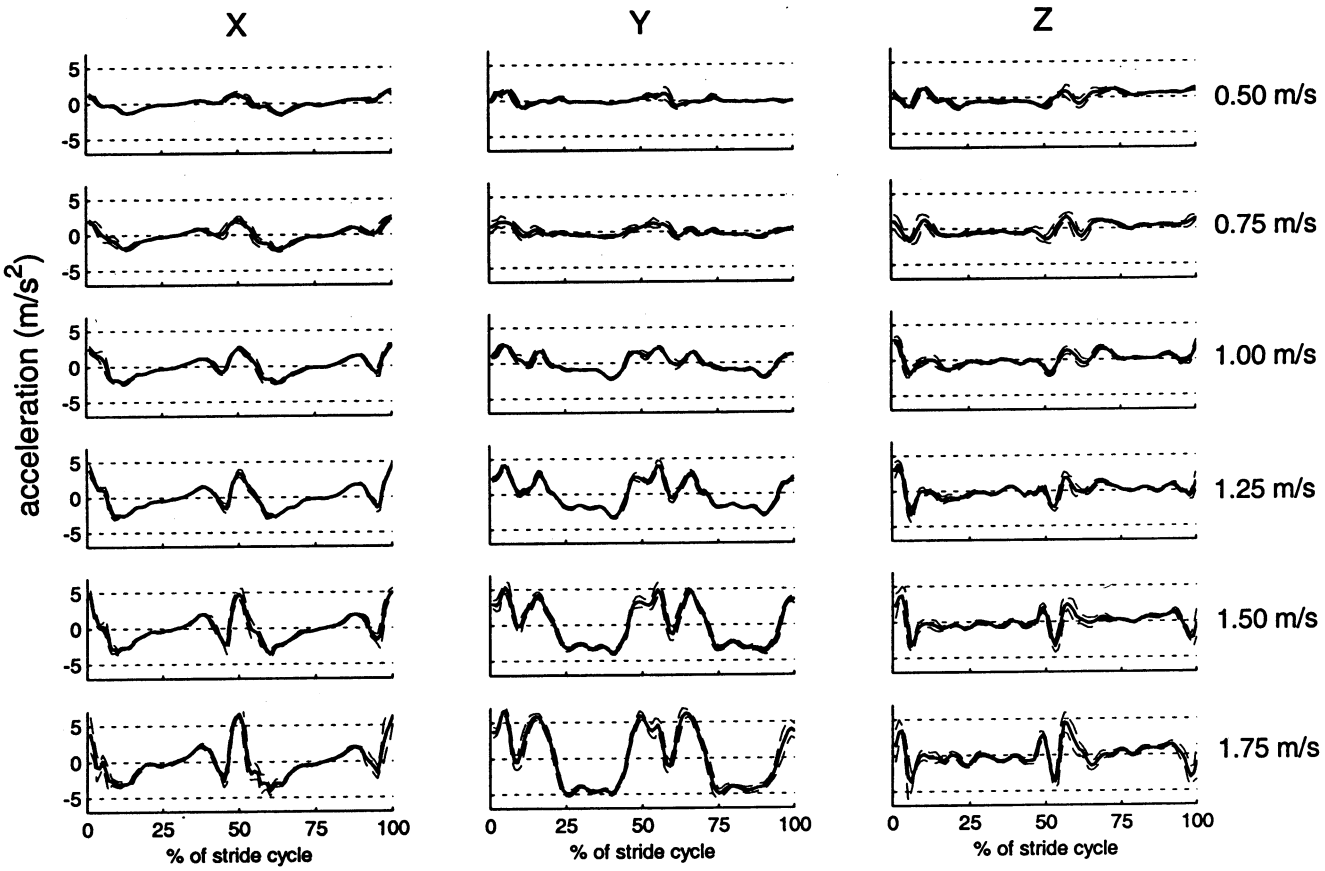

Fig. 1. Mean acceleration patterns of a male subject walking at different treadmill speeds. From top-to-bottom, the traces in each column show the effects of increases in treadmill speed from 0.5 to 1.75 m/s. The left column represents antero-posterior accelerations (X), middle column the vertical (Y), and right column the mediolateral accelerations (Z). Vertical accelerations are adjusted by subtracting the acceleration due to gravity (9.81 m/s^2). Solid lines represent mean patterns, and dashed lines represent ± 1 S.D. The stride cycle starts (0%) and ends (100%) with a right foot contact, left foot contact is at 50%.

with stride cycle duration, they are presented in Table 1. The reported mean differences illustrate the magnitude of systematic differences, whereas the standard deviations indicate random errors of the accelerometry-based methods when the GRF-based method is taken as a reference. The data in Table 1 show a decrease in stride cycle duration with increasing walking speed. With decreasing stride cycle duration, the mean differences between the GRF method and the zero-crossing method also decrease. However, differences between the GRF method and the peak detection method remain fairly constant, regardless of walking speed and stride cycle duration. Standard deviations do not show large differences between the zero-crossing and peak detection methods.

3.3. Discrimination between left and right steps

Fig. 3 shows left–right acceleration data and the calculated changes in position. Similar to the data in the figure, changes in mediolateral position, generally, had a sinusoidal shape. However, some exceptions were noted: in some subjects and some conditions the shape of the displacement pattern tended to a saw-tooth, and, particularly at higher speeds, a small contribution of higher harmonics could be observed. Nevertheless, the correspondence between the first harmonic and the left–right displacement pattern was moderate to good in most subjects and conditions; on average, the percentage of variance accounted for by the first harmonic was always more than 65%. Phase and amplitude of the first harmonic varied between subjects and with belt speed. In most subjects, the amplitude of the first harmonic was largest at low belt speeds. Thus, the group means decreased from 2.7 (at 0.50 m/s) to 1.5 cm (at 1.75 m/s). The observed variations in mean amplitude ranged between 6.5 and 0.2 cm. The mean phase decreased with speed from 32 to 6% of the stride cycle. However, at all speeds a between-subject variation in phase could be observed. In most of our data, left and right foot

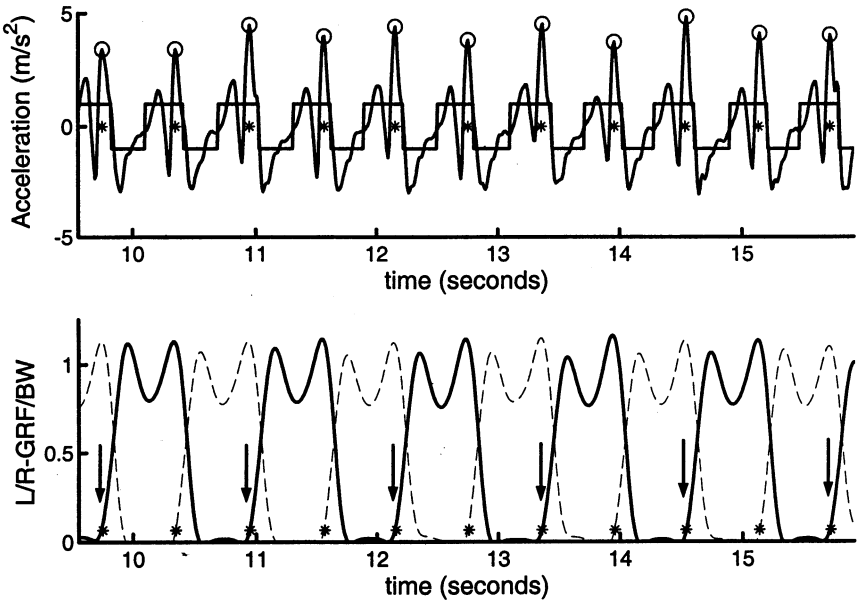

Fig. 2. Three methods of foot contact detection. Data traces represent a sample of the data of a male subject walking at a treadmill speed of 1.25 m/s. The upper figure shows antero-posterior acceleration data as a solid grey line. The lower figure shows right and left vertical GRFs (L/R-GRFs) divided by body weight (BW). Right GRFs are shown as a solid black line, and left GRFs as a dashed line. Arrows in the lower figure indicate the starts (and ends) of stride cycles, as identified by right GRFs. In both figures, asterisks indicate the instant of foot contact as detected from left or right GRFs. Foot contacts detected from acceleration data are indicated in the upper figure by downward slopes of the block signal shown in black (zero-crossing method), and the open circles around peak acceleration values (peak detection method).

contacts could be distinguished by their positive and negative values for the phase of the first harmonic. However, the distinction between left and right foot contacts was not always successful. In nine out of 15 subjects, a flawless distinction was possible for all foot contacts in all conditions. In the other six subjects (one male and five females), 12% of 756 foot contacts were labelled falsely. Particularly, in conditions where subjects walked with very small mediolateral displacements (i.e. mean amplitudes lower than 0.5 cm) a left–right distinction proved to be impossible. Such small amplitudes of mediolateral displacement were only observed in part of the data of three female subjects.

3.4. Estimated mean step length and mean walking speed during treadmill walking

Fig. 4 shows predictions of step length and walking speed versus real data for all subjects. The figure shows that the step lengths were underestimated in all subjects and at all speeds. Consequently, speed was underestimated as well. In the right part of Fig. 4, all predicted speeds were corrected by a multiplication factor of 1.25. After this correction, the mean differences between predicted and real speeds remained below ± 0.05 m/s. However, in individual data these differences could be larger: maximum differences increased with belt speed

Table 1
Stride cycle duration and differences between three methods of foot contact detection

Treadmill speed (m/s)	Stride cycle duration (s)		Time difference for GRFs versus zero-crossing method (s)		Time difference for GRFs versus peak detection method (s)	
	Mean	S.D.	Mean	S.D.	Mean	S.D.
0.50	1.744	0.164	− 0.103	0.025	0.002	0.027
0.75	1.430	0.105	− 0.083	0.016	− 0.013	0.019
1.00	1.242	0.082	− 0.065	0.014	− 0.015	0.016
1.25	1.135	0.072	− 0.053	0.011	− 0.011	0.011
1.50	1.063	0.064	− 0.037	0.012	− 0.003	0.012
1.75	0.984	0.061	− 0.026	0.012	0.003	0.011

Mean stride cycle duration was calculated from data obtained by the GRF method. Comparisons between the GRF method and two accelerometer-based methods (i.e. zero crossing and peak detection) represent mean and standard deviation of differences in timing. For further explanation see text.

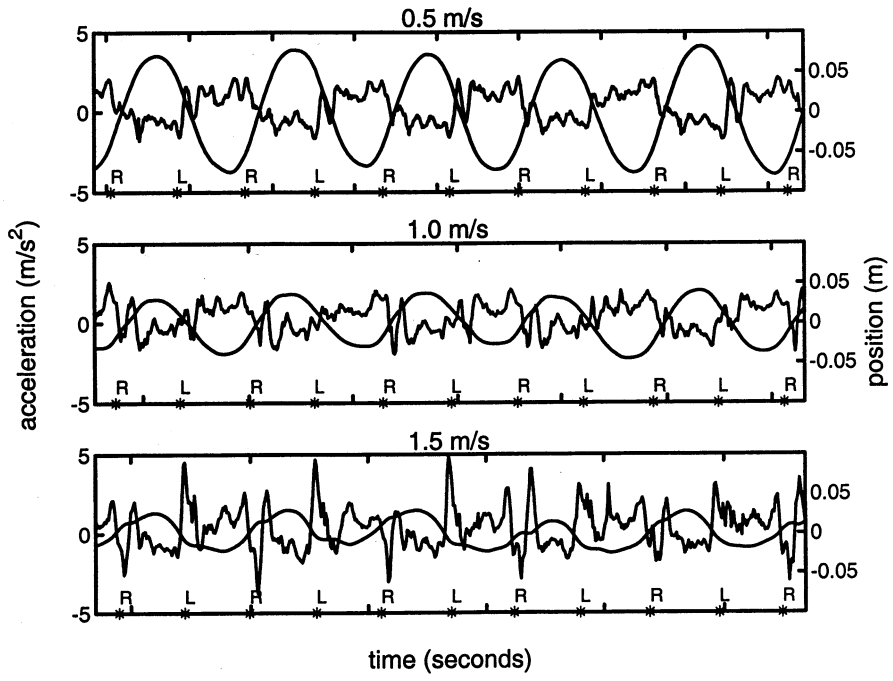

Fig. 3. Mediolateral accelerations and displacement patterns during five subsequent stride cycles. From top-to-bottom, data traces represent samples of a subject walking at treadmill speeds of 0.5, 1.0 and 1.5 m/s. Asterisks indicate the instant of foot contacts, as detected from left or right GRFs. Acceleration data are shown as solid grey lines and position data as solid black lines. L and R indicate the identification of the start of a left or right foot contact, respectively. In each box, the time scale is indicated by differences between tick marks, each representing 1 s.

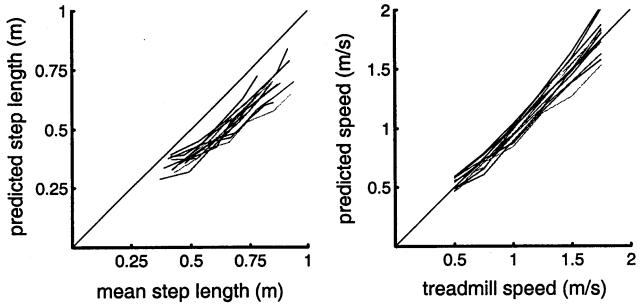

Fig. 4. Predicted step lengths and walking speeds during treadmill walking. The left figure shows predicted step length versus mean step length. The right figure shows predicted walking speed versus treadmill speed. In both figures, diagonal lines represent the situation where the prediction is equal to the data. The different lines represent the data of different subjects in all conditions.

from 0.08 (at 0.50 m/s) to 0.28 m/s (at 1.75 m/s). Thus, the maximum observed differences between predicted speed and treadmill speed remained lower than 16%. RMS errors increased with speed from 0.05 (at 0.50 m/s) to 0.14 m/s (at 1.75 m/s).

3.5. Spatio-temporal gait parameters during overground walking

Taking into consideration the results obtained in treadmill walking, only a peak detection method was used for foot contact detection during overground walking. Inspection of the forward acceleration signals and the detected foot contacts (analogous to the upper part of Fig. 2) revealed similar acceleration patterns as during treadmill walking, and no peaks were missed by the peak detection algorithm. Identification of left and right foot contacts was 100% successful in seven out of 10 subjects. However, similar to the results obtained during treadmill walking, a number of steps were labelled falsely in two female and one male subjects with small amplitudes of mediolateral movement. Fig. 5 shows predicted versus mean speeds during the three overground walking conditions. In correspondence with the results of treadmill walking, step lengths were underestimated during overground walking (not shown). The estimated speeds in Fig. 5 were obtained by applying the same multiplication factor (1.25) as before. After this correction, all but two estimated speeds remained within 15% of the calculated mean speed. The two exceptions were speed differences of 17.5 and 20%, respectively.

4. Discussion

The present paper investigated relationships between lower trunk accelerations and spatio-temporal gait parameters in male and female subjects. In the following, basic characteristics of the 3D-acceleration pattern will be discussed. Subsequently, it will be evaluated

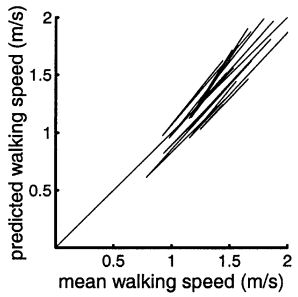

Fig. 5. Predicted walking speeds versus mean walking speeds during overground walking. The diagonal line represents the situation where the prediction is equal to the data. Different lines represent the data of different subjects during overground walking at three self-chosen speeds (slow, preferred and fast).

whether the instants of foot contacts, the distinction of left and right foot contacts, mean step length and walking speed can be determined from the accelerations of the lower trunk.

4.1. Trunk acceleration pattern

When analysing the mean acceleration patterns of the trunk, a number of observations can be made. First, an antero-posterior acceleration pattern has been found in which an acceleration during the later part of the support phase is followed by a deceleration shortly after foot contact (see Figs. 1 and 2, and Table 1). At all speeds, peak acceleration coincides with foot contact (see Table 1). Peak deceleration values are reached early after foot contact, and the change from deceleration to acceleration is reached halfway the step cycle (i.e. at approximately 25 and 75% of the stride cycle). Both peak acceleration and deceleration values increase with speed, but peak decelerations remain lower than peak accelerations. This basic pattern of forward acceleration corresponds to the pattern that can be expected based on inverted pendulum models of the CoM trajectory [16]. However, in some subjects, deviations from the basic pattern were observed, which varied from cycle to cycle and also with speed. Antero-posterior signals could show an additional acceleration or deceleration peak superposed on the basic acceleration pattern. Additional test trials where subjects were instructed to exaggerate their leg movements showed that these deviations from the basic pattern corresponded to the vehemence with which leg movements were accelerated or decelerated. Thus, the beginning or end of swing phases could show a peak or an indention, respectively. These additional peaks can be explained by the hip flexion or extension moments required for accelerating or decelerating the swing leg. As these hip moments also act on the pelvis, they influence the measured trunk accelerations.

Secondly, our data confirm the inverted pendulum prediction that left–right accelerations of the trunk are related to subsequent left and right foot placements (see Figs. 1 and 3). During the major part of a left support phase, the acceleration is to the right, and vice versa. However, these accelerations have small amplitudes, and during a support phase, the acceleration pattern can quickly change sign. The largest mediolateral accelerations are seen around the instant of foot contact; at right foot contact usually a short peak acceleration to the right, and at left foot contact a short peak acceleration to the left. These peaks increase with increasing speed, and they seem to be related to the medially directed impact of foot contacts. After these initial peaks, the acceleration changes sign, and usually the remainder of the support phase shows the pattern corresponding to the model prediction. Considering the large between-subject variability, the mediolateral accelerations seem to reflect idiosyncrasies of individual walking patterns. The latter are expressed in the mediolateral positioning of the foot but, during the support phase, also in the control of the hip abduction moment [20,21]. These two factors would contribute to both between- and within-subject variability in mediolateral accelerations.

Lastly, the vertical accelerations show a more complex pattern than the pattern that is expected based upon an inverted pendulum movement alone. Several factors may contribute to this complex pattern. First of all, the support moment generated in ankle, knee and hip joints of the support leg [22–24] contributes to the vertical accelerations. Peak acceleration values larger than gravity are reached shortly after foot contacts. With increasing walking speed, these upward acceleration peaks increase in amplitude. In addition, the data of most of our subjects start showing an indention between approximately 5 and 15% of the stride cycle. This indention roughly coincides with toe-off, and similar to the observed effects of leg movements on the forward accelerations, this indention could be caused by the leg movement during toe-off. After toe-off, the vertical acceleration is still larger than gravity, possibly related to a contralateral knee extension due to activity in the quadriceps muscle. After approximately 20% (and 70%) of the stride cycle, the vertical acceleration becomes smaller than gravity. The subsequent deceleration lasts until approximately 45% (and 95%) of the stride cycle. Both peak acceleration and deceleration values increase with speed. Deceleration periods in the vertical acceleration signals grow longer with increasing speed. They are related to the centripetal forces due to an almost circular trajectory over the support leg. Considering the distribution of leg length (l) within our group of subjects and the range of walking speeds (v), the effects of speed

on vertical acceleration (i.e. v^2/l) could, theoretically, range from about -0.25 to -2.75 m/s^2.

4.2. Trunk acceleration and spatio-temporal gait parameters

The results of the analysis of relationships between characteristics of trunk accelerations and spatio-temporal gait parameters reveal some promising possibilities in regard to gait analysis based on trunk accelerometry.

The comparison between different methods of foot contact detection shows that both the accelerometry-based methods show small errors in comparison to a reliable standard method using GRF data (see Table 1). Detection of foot contacts based upon a change of sign in forward acceleration data shows consistent differences with the GRF data. Although this zero-crossing method can perfectly be used for determining temporal gait parameters, a peak detection method must be preferred when movement patterns or muscle activity within the stride cycle are to be analysed. Contrary to a peak detection method, the "late" detection of foot contacts by the zero-crossing method affects the timing of patterns within the stride cycle. Thus, the use of the latter method would lead to (small) differences in timing in comparison to data presented in the literature.

After the instants of foot contact have been determined, the major part of left and right foot contacts can be distinguished based on mediolateral accelerations. Nevertheless, some reservation does apply. Because of the characteristics of mediolateral acceleration, we considered an analysis of changes in position better suited for an identification of left and right steps. However, due to the between-subject variation in timing, and in some cases, due to the very small amplitudes of left–right displacement, a valid detection was not possible in all conditions. In some cases, it may be difficult to get around these problems. However, when series of steps are to be analysed, not all left and right steps need to be identified successfully. When criteria for (non-) acceptance are defined, it suffices to identify a number of steps correctly and then to reconstruct whether a non-accepted step was a left or right step.

Apart from the determination of temporal gait parameters, we also attempted to estimate step lengths and mean walking speed. Our results show that crude estimations of mean step length and walking speed are possible based on lower trunk accelerations. In these estimations, we did not need more information than the measured accelerations and leg length. Although possibilities exist to optimise individual predictions and obtain more accurate estimations of mean step length and walking speed, the attractiveness of a rather simple (but crude) estimation would be lost.

In this study, we used a treadmill for analysing the relationships between lower trunk acceleration and spatio-temporal gait parameters because a reliable standard method was needed. The treadmill used in this study had an important advantage that GRFs under the left and right foot could be collected separately. Through the availability of left and right GRFs, we obtained a reliable indication of subsequent foot contacts. Thus, an evaluation of the accelerometry-based methods was possible using a large number of consecutive stride cycles. As was expected based upon the biomechanics of treadmill and overground locomotion [25], our study shows similar results in these two conditions. The results obtained for overground walking demonstrate that the presented methods can be usefully incorporated in methods for studying gait under real-life conditions. However, since the proposed methods assume an inverted pendulum-like behaviour during walking in an approximately straight line, applying the same methods when subjects walk with sharp left or right turns, or abruptly speed up or slow down, might influence the results.

In conclusion, this paper describes and discusses some basic mechanisms underlying the pattern of lower trunk accelerations during walking. An analysis of these patterns shows that it is possible to obtain a good identification of stride cycles and (left and right) steps from the acceleration data, and reasonable approximations of mean step length and walking speed.

Acknowledgements

This study was financially supported by the Ministry of Economical Affairs (BTS Grant NR 98206). The author would like to thank Koen Vaartjes and Sander Heikens for technical assistance.

References

[1] Zijlstra W, Rutgers AWF, Hof AL, Van Weerden TW. Voluntary and involuntary adaptation of walking to temporal and spatial constraints. Gait Posture 1995;3:13–8.
[2] Nilsson J, Thorstensson A. Adaptability in frequency and amplitude of leg movements during human locomotion at different speeds. Acta Physiol Scand 1987;129:107–14.
[3] Zijlstra W, Rutgers AWF, Van Weerden TW. Voluntary and involuntary adaptation of gait in Parkinson's disease. Gait Posture 1998;7:53–63.
[4] Nevill AJ, Pepper MG, Whiting M. In-shoe pressure measurement system utilising piezoelectric film transducers. Med Biol Eng Comput 1995;33:76–81.
[5] Zijlstra W, Dietz V. Adaptability of the human stride cycle during split-belt walking. Gait Posture 1995;3:250–7.
[6] Verkerke GJ, Ament W, Wierenga R, Rakhorst G. Measuring changes in step parameters during an exhausting running exercise. Gait Posture 1998;8:37–42.

[7] Klenerman L, Dobbs RJ, Weller C, Leeman AL, Nicholson PW. Bringing gait analysis out of the laboratory and into the clinic. Age Ageing 1988;17:397–400.
[8] Huitema RB, Hof AL, Postema K. Ultrasonic motion analysis system—measurement of temporal and spatial gait parameters. J Biomech 2002;35:837–42.
[9] Morris JRW. Accelerometry—a technique for the measurement of human body movements. J Biomech 1973;6:729–36.
[10] Hayes WC, Gran JD, Nagurka ML, Feldman JM, Oatis C. Leg motion analysis during gait by multi-axial accelerometry: theoretical foundations and preliminary validations. J Biomech Eng 1983;105:283–9.
[11] Willemsen AT, van Alste JA, Boom HB. Real-time gait assessment utilising a new way of accelerometry. J Biomech 1990;23:859–63.
[12] Moe-Nilssen R. A new method for evaluating motor control in gait under real-life environmental conditions. Part 2: gait analysis. Clin Biomech 1998;13:328–35.
[13] Aminian K, Robert P, Jequier E, Schutz Y. Incline, speed, and distance assessment during unconstrained walking. Med Sci Sports Exerc 1995;27:226–34.
[14] Aminian K, Rezakhanlou K, De Andres E, Fritsch C, Leyvraz PF, Robert P. Temporal feature estimation during walking using miniature accelerometers: an analysis of gait improvement after hip arthroplasty. Med Biol Eng Comput 1999;37:686–91.
[15] Willemsen AT, Bloemhof F, Boom HB. Automatic stance-swing phase detection from accelerometer data for peroneal nerve stimulation. IEEE Trans Biomed Eng 1990;37:1201–8.
[16] Zijlstra W, Hof AL. Displacement of the pelvis during human walking: experimental data and model predictions. Gait Posture 1997;6:249–62.
[17] Wu G, Cavanagh PR. ISB recommendations for standardization in the reporting of kinematic data. J Biomech 1995;28:1257–60.
[18] Shimba T. An estimation of centre of gravity from force platform data. J Biomech 1984;17:53–60.
[19] McKinnon CD, Winter DA. Control of whole body balance in the frontal plane during human walking. J Biomech 1993;26:633–44.
[20] Winter DA. Human balance and posture control during standing and walking. Gait Posture 1995;3:193–214.
[21] Otten E. Balancing on a narrow ridge: biomechanics and control. Philos Trans R Soc Lond B 1999;354:869–75.
[22] Winter DA. Overall principle of lower limb support during stance phase of gait. J Biomech 1980;13:923–7.
[23] Winter DA. Kinematic and kinetic patterns in human gait: variability and compensating effects. Hum Mov Sci 1984;3:51–76.
[24] Hof AL. On the interpretation of the support moment. Gait Posture 2000;12:196–9.
[25] Van Ingen Schenau GJ. Some fundamental aspects of the biomechanics of overground versus treadmill locomotion. Med Sci Sports Exerc 1980;12:257–61.